

Effect of randomizers on the power spectrum excess of space telemetry signals

Original

Effect of randomizers on the power spectrum excess of space telemetry signals / Battaglioni, M.; Baldi, M.; Chiaraluce, F.; Garelo, R.; Calzolari, G. P.; Vassallo, E.. - In: INTERNATIONAL JOURNAL OF SATELLITE COMMUNICATIONS AND NETWORKING. - ISSN 1542-0973. - ELETTRONICO. - 40:2(2022), pp. 67-82. [10.1002/sat.1416]

Availability:

This version is available at: 11583/2970407 since: 2022-08-01T09:14:33Z

Publisher:

John Wiley and Sons Ltd

Published

DOI:10.1002/sat.1416

Terms of use:

This article is made available under terms and conditions as specified in the corresponding bibliographic description in the repository


Publisher copyright

(Article begins on next page)

ORIGINAL PAPER

WILEY

Effect of randomizers on the power spectrum excess of space telemetry signals

Massimo Battaglioni¹ | Marco Baldi¹ | Franco Chiaraluce¹ |
Roberto Garello²  | Gian Paolo Calzolari³ | Enrico Vassallo³

¹CNIT, DII, Università Politecnica delle Marche, Ancona, Italy

²DET, Politecnico di Torino, Turin, Italy

³ESOC, European Space Agency, Darmstadt, Germany

Correspondence

Massimo Battaglioni, CNIT, DII, Università Politecnica delle Marche, Ancona, Italy.
Email: m.battaglioni@staff.univpm.it

Funding information

European Space Agency

Summary

This paper presents a thorough analysis of the spectral characteristics of space telemetry signals when randomizers are used to counter the power excess, that is, the increase of the power spectrum in some measurement bandwidths with respect to the transmission of an ideal random signal. We show that a long randomizer actually improves the spectral characteristics but is not able to solve some critical problems appearing when all-zero frames or almost constant data are transmitted. Suitable solutions are proposed to face these cases, ensuring a small power excess in all possible operation conditions. The impact of high-order modulations and error correcting codes is also investigated.

KEYWORDS

power spectrum, randomizer, space links, telemetry

1 | INTRODUCTION

The power flux density (PFD) at the Earth's surface produced by emissions from a spacecraft cannot exceed prefixed values, for all conditions and methods of modulation. In particular, this is true for the space telemetry (TM) signals, whose purpose is to reliably and transparently convey measurement information from a data source located in space to users located on Earth.¹

More precisely, the International Telecommunication Union (ITU) regulates radiocommunication services and utilization of radio frequencies on law of nations scale. As part of the ITU Radio Regulations Article 21 Section V,² ITU establishes the PFD limits concerning transmissions from space to Earth. At the Earth's surface, the PFD produced by space station emissions shall not exceed the limits provided in International Telecommunication Union² on a given measurement bandwidth, which is 4 kHz for the 8-GHz band and 1 MHz for the 26-GHz band.

A critical aspect of compliance with PFD limits is represented by the actual shape of the received power spectrum. In fact, space links are usually designed under the assumption of random binary information sequences, producing ideal and continuous spectra, with some fixed margin to take into account nonidealities. The margin is usually introduced in a heuristic way: 6 dB is a typical value used in many missions. In practice, however, ideal randomness does not exist, as real data always exhibit some form of correlation. To improve the randomness of the transmitted binary sequences and approach the ideal behavior, data randomizers are used. However, if the randomizer performance is suboptimal, the transmitted power spectrum may still show some peaks over the ideal level, that is, some power excesses. In particular, when some special, that is, constant or nearly constant, transfer frames (TFs) are transmitted, nonideal randomization may induce a very high power excess in some measurement bandwidths.³

Violations of the ITU PFD limits, when detected, automatically result in a request to switch off transmission over the territory of the station experiencing harmful interference. Measuring the PFD for Earth exploration satellites passing over the same part of the world many times per day

This is an open access article under the terms of the [Creative Commons Attribution-NonCommercial-NoDerivs](https://creativecommons.org/licenses/by-nc-nd/4.0/) License, which permits use and distribution in any medium, provided the original work is properly cited, the use is non-commercial and no modifications or adaptations are made.

© 2021 The Authors. *International Journal of Satellite Communications and Networking* published by John Wiley & Sons Ltd.

is a very easy task that can be accomplished with high accuracy. This was done, for example, with the ENVISAT satellite, operated by the European Space Agency (ESA), for which the unexpected 6-dB violation of PFD limits during modes transition was measured by a monitoring station in Germany several years ago. An example of the measured peaks is shown in Figure 1A. Thanks to the satellite on-board flexibility, a software patch could be developed, uploaded, and successfully demonstrated to the European Conference of Postal and Telecommunications Administrations (CEPT), so that operations of ENVISAT could continue. The measured spectrum after on-board modification is shown in Figure 1B. In light of this experience, ESA developed the follow-on SENTINEL-1/2/3/5P fleet consisting of 10 satellites spanning 25 years of expected lifetime with proprietary randomizers to avoid this problem. The importance of this issue increases every year with the constant increase of on-board instruments resolution and of latency requirement yielding increased data rates for transmission and requiring higher order modulations to comply with the available channel bandwidth. To cope with these constraints, the links are designed to just meet the PFD limits under ideal conditions. In this paper, we show some examples where nonrandom data effects can easily increase the PFD by 6 dB or more, which would require reducing the transmit power by the same amount, thus reducing the data rate by a factor of 4 or more. In such a framework, most space agencies agreed to develop an open international standard as opposed to proprietary solutions, so that cross support is made possible.

Typical randomizers are based on linear feedback shift registers (LFSRs). When maximum-length LFSRs are used, M-sequences generated by LFSRs are nearly ideal. Unfortunately, very often, the randomizer does not exploit the entire period (or an integer multiple of the period) of the LFSR-generated sequence, but only a portion (or an integer multiple of the period plus a portion) of it, according to the length of the binary information frame. In this case, truncated M-sequences lose their optimal properties and a significant spectrum power excess may show up.⁴

Based on the above premises, it is important to know by how many dBs the real spectrum of the received signal will exceed the spectral level of an ideal random signal. In order to satisfy the PFD limits, such a power excess must be taken into account in the link budget computation, because the margins with respect to the ITU limits have to overcome such a power excess. Thus, a large power excess yields large margins (as said above, to be sure that the ITU PFD limits are satisfied), with negative consequences on the system link budget, design, and performance.

As concerns the randomizer, the one currently recommended by the Consultative Committee for Space Data Systems (CCSDS) in TM links is based on a quite short eight-cell LFSR⁵ and will be denoted as *eight-cell randomizer* afterward. As pointed out by the Centre National d'Etudes Spatiales (CNES) some years ago, the performance of this randomizer may degrade when high data rates and long size telemetry frames are used.⁶ To address this issue, CNES proposed to adopt a 15-cell LFSR taken from the DVB-S2⁷ standard and able to achieve better performance than the eight-cell randomizer. In some previous papers,^{3,4,8} we investigated the properties of both these randomizers, with special emphasis on the analysis of truncated LFSR sequences and their impact on the spectrum and the power margin. Moreover, we proposed some possible solutions to cope with only-idle frames and the corresponding power excess. The topic has recently been revitalized by the National Aeronautics and Space Administration (NASA), that has proposed a new randomizer composed of 17 cells,^{9–11} which will be denoted as *17-cell randomizer* afterward. Consequently, ESA has started studying such a new randomizer, with the goal to verify its ability to improve the performance of the eight-cell randomizer, thus paving the way for a possible update of the current recommendations for TM transmissions.

In this paper, we summarize the main results obtained by such a study. In particular, we show that the longer randomizer is indeed able to reduce the power excess when only-idle frames are transmitted but, at high bit rates, this reduction may be not sufficient to bring the power excess below practical design margins. To overcome this problem, we propose to adopt a different randomizer to be used to generate only-idle frames, and we show that the resulting power spectra exhibit much more favorable behaviors. As concerns normal TM data frames, they usually

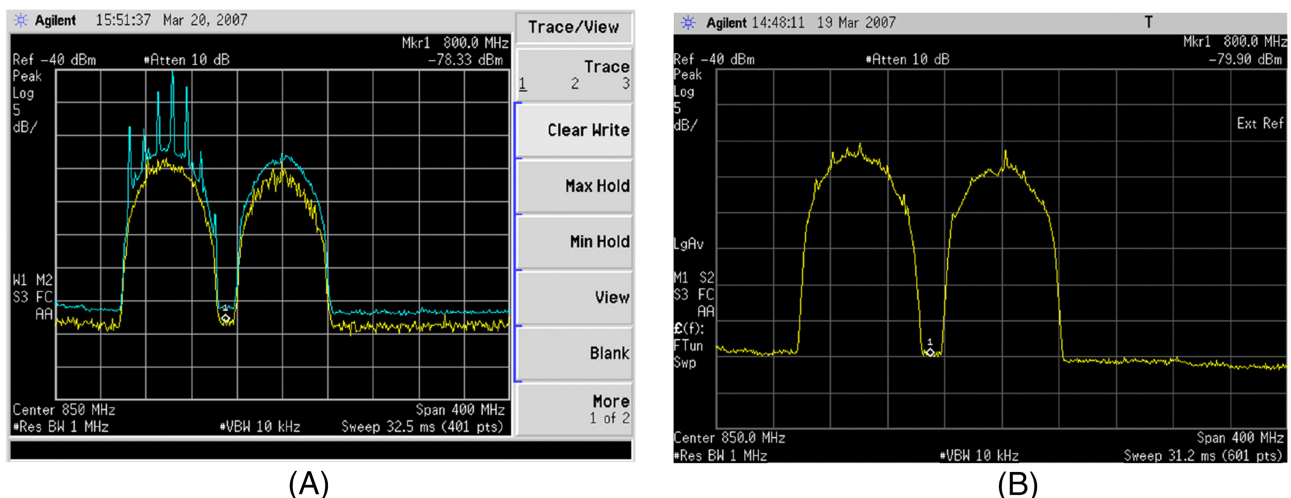


FIGURE 1 Experimental evidence of the power spectrum excess. (A) Measured ENVISAT spectrum. (B) Measured ENVISAT spectrum after on-board modification

exhibit a “random-like” behavior and thus do not exhibit significant power excesses. However, if their randomness is below usual and the bits are almost constant for a rather long period of time, this is no longer true. Then, we also investigate the spectral properties of almost constant frames at high data rates. Finally, we consider the impact of high-order modulations and error correcting codes, thus providing a complete analysis of the telemetry signal spectral properties in realistic conditions.

It must be noted that the peaks in the spectrum we are dealing with in this work are not due to nonlinear phenomena like those occurring, for example, in high power amplifiers. Instead, the peaks we consider are due to the (nonideal) random properties of the transmitted sequences. Hence, they cannot be addressed by using pre-distortion techniques that are used to mitigate spurious emissions due to nonlinear effects in conventional communications.¹²

The organization of the paper is as follows. In Section 2, the structure and the main properties of the eight-cell randomizer and 17-cell randomizer are described. In Section 3, the main features of the telemetry signal spectrum are discussed, together with the methodology to compute it and evaluate the power excess. In Section 4, some results are presented, considering different scenarios and operation conditions. Finally, some conclusions are drawn in Section 5.

2 | STRUCTURE AND STATISTICAL PROPERTIES OF RANDOMIZERS

The eight-cell randomizer currently included in the CCSDS recommendation for TM synchronization and channel coding⁵ uses the LFSR with $M = 8$ cells shown in Figure 2, where $s(i)$, with $i = 1, \dots, M$, represents the content of the i th cell. The connections (1, 3, 5, 8), corresponding to the primitive polynomial $D^8 + D^7 + D^5 + D^3 + 1$, guarantee the generation of a maximum-length sequence with period $N = 2^8 - 1 = 255$ bits. All the LFSR cells are preset to 1 at the beginning of each frame, and then the randomized version of each frame is obtained as the bit-wise sum of the frame itself with the LFSR output sequence. Hence, the LFSR sequence summed to each frame is always the same. This is a very popular choice for practical applications because it allows acquiring both frame and LFSR synchronization simultaneously.

In order to address power excess problems, it has recently been proposed by NASA to replace the eight-cell randomizer reported in Figure 2 with the 17-cell randomizer shown in Figure 3. Its primitive polynomial is $D^{17} + D^{14} + 1$, which guarantees the generation of a maximum-length sequence with period $N = 2^{17} - 1 = 131071$ bits. The binary sequence 11000111000111000 has been suggested as a starting seed to be reset at the beginning of each frame and will be considered in the following.

When evaluating the performance of a randomizer, the following metrics are commonly evaluated:

- the 0/1 distribution, that is, the probability of having bits 0 or 1;
- the transition distribution, that is, the probability of having a bit transition (from 0 to 1 and vice versa) in any position;
- the run distribution, that is, the probability of having sequences of consecutive equal bits (called runs);
- the periodic autocorrelation function (AF), whose definition will be reminded next.

Indeed, the values of these parameters when using the complete M-sequences produced by an LFSR are well known from the theory. What is relevant is that they comply with the constraints of practical space systems. In particular, in Consultative Committee for Space Data Systems,¹³ it is recommended that

- the maximum run length of either consecutive ones or consecutive zeros is limited to 64 bits;

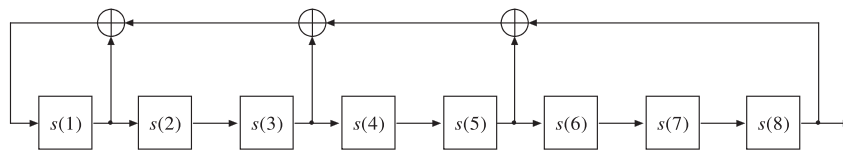


FIGURE 2 The eight-cell Consultative Committee for Space Data Systems (CCSDS) randomizer

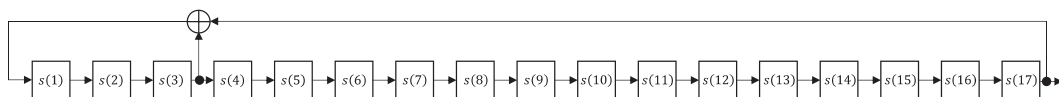


FIGURE 3 The 17-cell National Aeronautics and Space Administration (NASA) randomizer

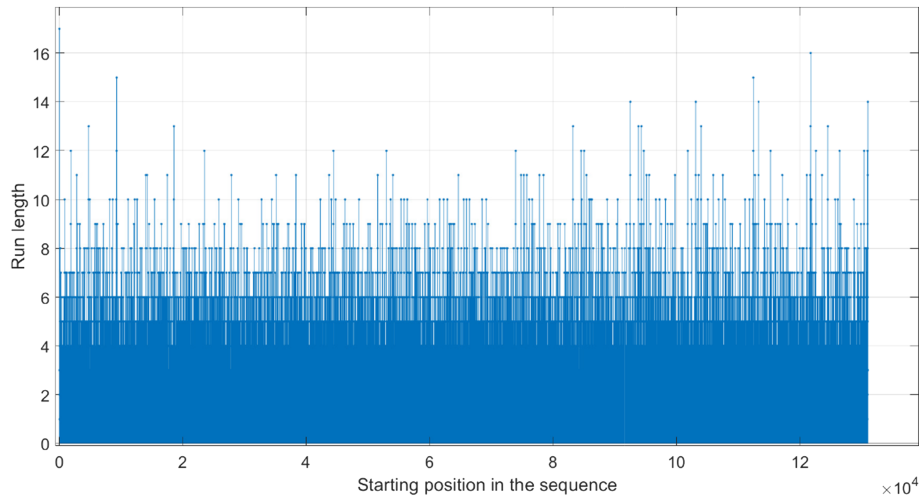


FIGURE 4 Run length evolution for the 17-cell randomizer

- for near Earth missions (having an altitude above the Earth smaller than 2.0×10^6 km), a minimum of 125 transitions occur in any sequence of 1000 consecutive symbols; for deep space missions (having an altitude above the Earth larger than, or equal to, 2.0×10^6 km), a minimum of 275 transitions occur in any sequence of 1000 consecutive symbols. These values were determined to keep the ground demodulators locked.

Such constraints are widely satisfied by the mentioned randomizers. In fact, for an M-sequence produced by any LFSR with M cells, the maximum run length is M for the complete sequence and at most $2M - 2$ for the truncated one (considering nontrivial lengths, that is, larger than M), regardless of the seed. This means that run lengths are not larger than 8 and 14, respectively, for the eight-cell randomizer, and not larger than 17 and 32, respectively, for the 17-cell randomizer. Similarly, it is possible to verify that the number of transitions every 1000 symbols is about 500, that is, significantly larger than 125 and 275, for both randomizers.

The run length evolution (length of the runs occurring from the beginning to the end of the sequence) on the entire period N of the 17-cell randomizer is shown in Figure 4. It is interesting to observe that by appropriately changing the starting seed (which causes a cyclic shift of the LFSR sequence), it is possible to avoid the appearance of long runs in case of relatively short frames, that is, not using the entire LFSR sequence.

For the correlation properties, we consider the so-called *periodic AF*, as it is of interest in the evaluation of the power spectrum. Given a sequence of length F , by assuming bipolar symbols $b_i \in [-1, +1]$, the periodic AF is defined as

$$R(i) = \sum_{k=0}^{F-1} b_k b_{k+i} \quad (1)$$

where $0 \leq i < F$ and $k + i \equiv (k + i) \bmod F$ (the sequence is viewed as infinite, with period F). If $F = N$, that is, the entire M-sequence length is considered, then $R(i) = -1, \forall i \in [1, N-1]$. Conversely, as known in the literature and widely discussed in Baldi et al.,⁸ for $F < N$, the M-sequence is truncated and the AF may exhibit a significantly different behavior. Examples are shown in Figure 5 for both the eight-cell randomizer and the 17-cell randomizer. The huge truncation considered for the 17-cell randomizer takes into account that, according to Consultative Committee for Space Data Systems,⁵ the TF length is any integer number of octets with a maximum of 2048 octets.¹ If instead $F > N$, the computation is extended over more than one M-sequence period.

A very relevant parameter when analyzing the AF features is the maximum peak side lobe (MPSL), defined as the largest absolute value of the out-of-phase AF. Again with reference to the case of $F \leq N$, we have

$$\text{MPSL} = \max_{i \neq 0} |R(i)|. \quad (2)$$

For an ideal, non-truncated, maximum-length sequence, we obviously have $\text{MPSL} = 1$, while for a truncated sequence the MPSL may be significantly larger. The MPSL behavior, as a function of the number of bits of truncation, is shown in Figure 6 for both the eight-cell randomizer and

¹For the sake of completeness, however, it must be said that the maximum TF length will be increased to 64,000 octets after adoption of the Unified Space Data Link Protocol (USLP).¹⁴

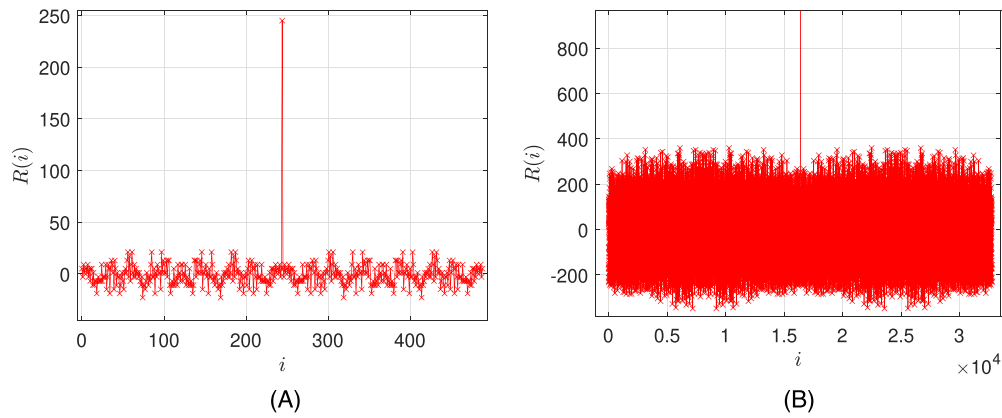


FIGURE 5 Examples of autocorrelation function (AF) for truncated linear feedback shift register (LFSR) sequences: (A) eight-cell randomizer with 10 bits of truncation and (B) 17-cell randomizer with 114,687 bits of truncation

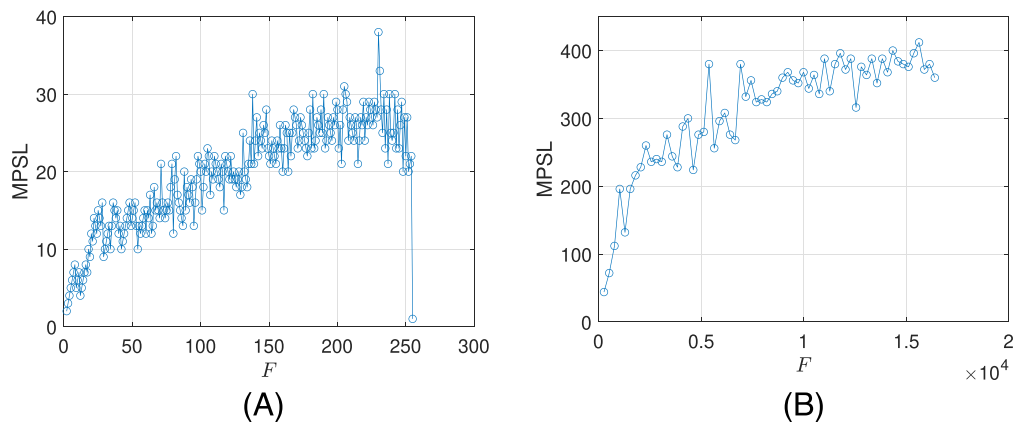


FIGURE 6 Maximum peak side lobe (MPSL) for truncated linear feedback shift register (LFSR) sequences as a function of the number of bits of truncation: (A) eight-cell randomizer and (B) 17-cell randomizer

the 17-cell randomizer. Our main interest is in the evaluation of the impact of these large values of MPSL on the power spectrum. This is done in the following sections.

2.1 | Telemetry TFs

We consider two types of transmitted TFs:

- Frames containing science and spacecraft housekeeping data, simply called data in the rest of the paper. Usually, these frames already have good randomness characteristics. (Almost constant frames will be considered in the following, too.)
- Only-idle data (OID) frames, which are used to fill the bit streaming when no frames are available. Typically, they are filled with all-zero bits and, for this reason, they are definitely nonrandom.

For any TF, the data (or the OID) are preceded by a header, which contains identification, sequence control, and packet length information (see Consultative Committee for Space Data Systems¹⁵ for details). The impact of the header, whose contents slightly change from frame to frame, is negligible; thus, we will not consider its exact structure in the following.

We will denote the TF length by the symbol L . The TF (optionally encoded through a suitable error correcting code, whose impact will be investigated in Section 4.4) is EX-ORed with one or more repetitions of the LFSR sequence, truncated when necessary, and preceded by a 32-bit attached sync marker (ASM), which is required for frame synchronization. The resulting packet, named channel access data unit (CADU) in the

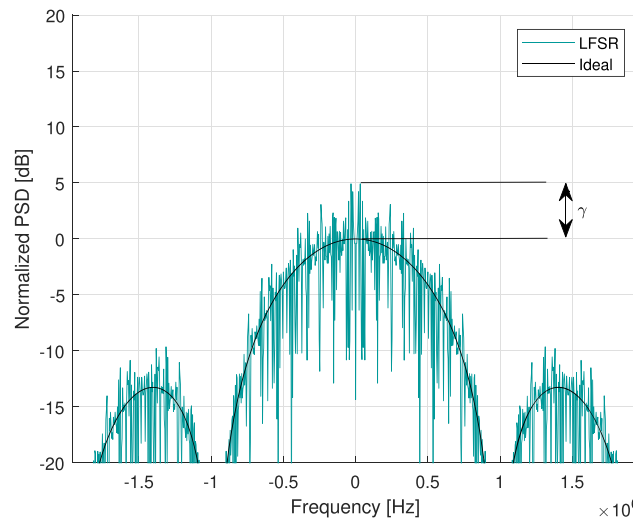


FIGURE 7 Example of comparison between ideal and actual received spectrum with power excess

following, is $L_T = L + 32$ bits long in absence of forward error correction coding. For the purposes of our study, the role of the ASM is very limited and will be often neglected. The ASM impact will be addressed in Section 4.3.

3 | POWER SPECTRUM

ITU PFD limits are referred to the power received inside a measurement bandwidth B , and we focus on $B = 4$ kHz. Thus, for all the nonideal spectrum figures presented in the following, each point represents the power received inside a frequency bin of B Hz. An example is shown in Figure 7. The black curve represents the ideal spectrum; this curve is always conventionally shifted up to have its maximum at 0 dBW; this corresponds to normalize the spectrum, as shown in the figure. The irregular curve (noted as LFSR) is the actual received spectrum. Each y axis value denotes the power received inside the measurement bandwidth with central frequency corresponding to the x axis value. Peaks above the ideal curve show that, in some bins, we receive more power with respect to the ideal case; that is, a power excess appears. The maximum power excess in a bin, noted by γ , is the largest difference between the violet curve and the maximum of the ideal curve (i.e., 0 dB in our figures). It is important to remark that it is not necessarily the largest difference between the two curves, because ITU limits are expressed in terms of maximum absolute, not relative, power in a bin.

3.1 | The role of peaks separation

Let us suppose to transmit a sequence of OID frames with all-zero bits. As mentioned above, the LFSR randomizer is reset at the beginning of each frame; then, the OID of the transmitted CADUs are always the same. In this condition, an almost² periodic sequence with period $P \leq L_T$ is transmitted. The period is smaller than L_T when the length of the LFSR sequence, N , is smaller than L_T (or smaller than L when the ASM is neglected).

Let us denote by R_b the bit rate, expressed in bits per second (bps) and suppose to use binary phase shift keying (BPSK) modulation. The power spectral density (PSD) is obtained as the Fourier transform of the AF; then, because of the almost periodic feature, in order to have an idea of the problem, we can approximate the spectrum with a sequence of Dirac delta functions having

- separation $\Delta = R_b/P$ (Hz) and
- area dependent on the local value of the AF.

²The sequence is not exactly periodic because of the presence of the variable header that however, as mentioned, has a negligible impact.

According to current regulations, we must evaluate the power received into bins of bandwidth B . For such a purpose, let us compare the separation Δ with the measurement bandwidth B . We can distinguish two cases. If $\Delta > B$, some bins do not contain any Dirac delta, while some others contain one Dirac delta and are those in which we can expect a significant power excess. Conversely, if $\Delta \leq B$ there are one or more Dirac deltas inside each bin: this is a more favorable situation because the distribution of power across bins is more uniform, although some bins may still have a power excess. Clearly, the first case is the most dangerous one, because the risk of having a significant value of the maximum power excess in a bin is high. Nevertheless, we can have a large value of γ also in the second case, depending on the bit rate and the AF behavior. Then, we conclude that the condition of having a separation Δ smaller than the measurement bandwidth B is neither a necessary nor a sufficient condition to have small peaks, even if this condition corresponds, in principle, to a more favorable situation.

3.2 | Methodology

Given a binary sequence for which we want to assess the corresponding power spectrum, we can choose the observation window W , which defines the amount of time for which we collect the samples of the received signal and use one of the following methods:

1. Apply Bartlett's method and average over x different periodograms computed on the x consecutive frames received inside the window W .
2. Compute the periodogram on the entire window W to obtain a higher frequency resolution and then accumulate the power received inside the measurement bandwidth B .

The two methods above produce equivalent results. We have applied the second one, by computing a single fast Fourier transform (FFT) on the entire frame and then summing the power contributions to obtain the value received in each bin with bandwidth B . The analysis can be done in baseband, because the introduction of the carrier only corresponds to shifting the spectrum at higher frequencies. For this reason, the spectra are plotted around the zero frequency while, in reality, they are centered on the carrier frequency.

Therefore, in order to analyze the spectrum of the binary sequences, we first map them into signals whose shape depends on the chosen modulation. Then we sample them, we compute their AF and, finally, their Fourier transform to obtain the PSD. As an alternative, as known from signal theory, we might compute the squared modulus of the Fourier transform of the sampled sequence. This gives us a frequency resolution that depends on both the symbol rate and the number of symbols inside the considered observation window W . Given this frequency resolution, we compute the power contained inside each measurement bandwidth B .

It is important to understand the role of the observation window for random and nonrandom sequences. When sequences of equal frames are transmitted, the spectral properties do not depend on the chosen observation window W but only on the sequence structure. Thus, in such a case, we obtain the same results in terms of power received in a bin for any choice of W (obviously W must be large enough to have a frequency resolution of at least B Hz).

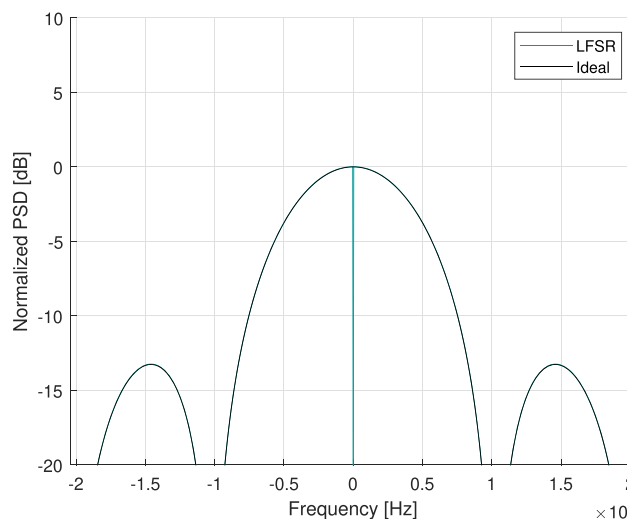


FIGURE 8 Example of power spectrum for a sequence produced by the eight-cell randomizer with $R_b = 1.02$ Mbps, $L = N = 255$ bits, $B = 4$ kHz, only-idle data (OID) channel access data unit (CADU) with all-zero bits

Instead, when sequences of random frames are transmitted, the choice of the observation window W becomes important. Power spectra are observed by swept spectrum analyzers (where a band-pass filter with bandwidth equal to the measurement bandwidth is swept along the frequency axis), or FFT-based spectrum analyzers (which collect signal samples inside a time window, compute the FFT and plot it on the screen). In this case, the observation window must be large enough to observe a stable spectrum. Note that by using Bartlett's method (or, equivalently, averaging over consecutive frequency samples), we have a spectrum whose precision increases with W . Very large values of W , however, yield very long simulation times, and some trade-off must be found in such a way as to obtain sufficiently precise results in an acceptable simulation time. Taking into account these issues, in our evaluation we have chosen an observation window $W = 100$ ms, except for a couple of cases that will be clearly indicated in the following.

3.3 | Preliminary examples

To illustrate the impact of the peaks separation in a real (not theoretical) scenario, some examples are shown in Figures 8–10, referred to the eight-cell randomizer without considering the ASM. In Figure 8, the peaks separation is $\Delta = 4$ kHz, that is, equal to the measurement bandwidth;

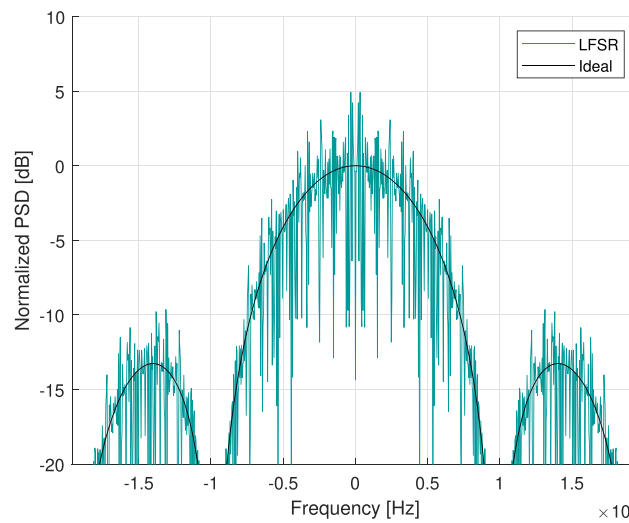


FIGURE 9 Example of power spectrum for a sequence produced by the eight-cell randomizer with $R_b = 0.98$ Mbps, $L = 245$ bits, $B = 4$ kHz, only-idle data (OID) channel access data unit (CADU) with all-zero bits

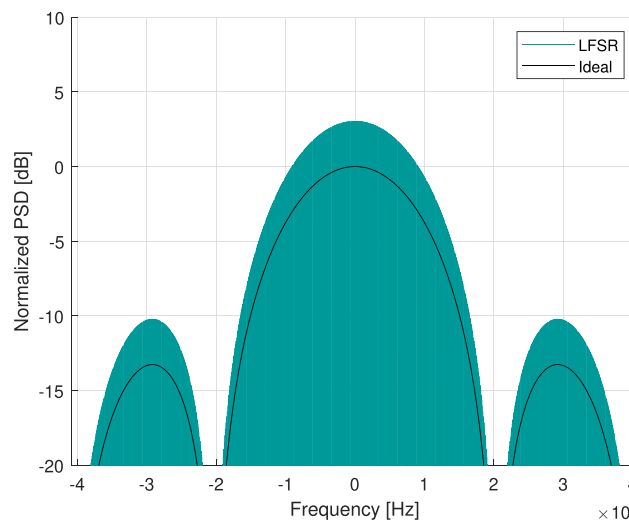


FIGURE 10 Example of power spectrum for a sequence produced by the eight-cell randomizer with $R_b = 2.04$ Mbps, $L = N = 255$ bits, $B = 4$ kHz, only-idle data (OID) channel access data unit (CADU) with all-zero bits

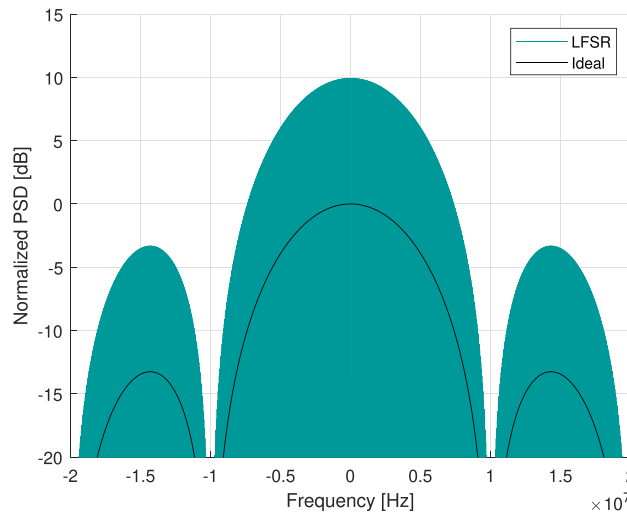


FIGURE 11 Example of power spectrum for a sequence produced by the eight-cell randomizer with $R_b = 10$ Mbps, $L = 10,000$ bits, $B = 4$ kHz, only-idle data (OID) channel access data unit (CADU) with all-zero bits, no attached sync marker (ASM)

the frame length covers the entire LFSR period and, in this condition, the AF is nearly ideal. As a consequence, the spectrum shape is ideal as well, and we have $\gamma \approx 0$ dB. In Figure 9, we show the impact of truncation: we have $\Delta = B = 4$ kHz again, but in this case, the LFSR sequence is truncated 10 bits before its end. As a consequence, a significant power excess appears and $\gamma \approx 5$ dB. Finally, in Figure 10, we show the impact of the bit rate: $\Delta = 2B = 8$ kHz and, although $L = N$ and the spectrum shape is ideal, we have $\gamma \approx 3$ dB.

4 | NUMERICAL RESULTS

As already mentioned, the main power excess issues occur when OID frames with all-zero bits are transmitted. So we mainly focus on this scenario in the following. Figure 11 shows the power spectrum for the eight-cell randomizer sequence assuming $R_b = 10$ Mbps and $L = 10,000$ bits. Because the period of the LFSR sequence is (much) smaller than L , the peaks separation is determined by $P = N$ and results in $\Delta \approx 39$ kHz. The corresponding power excess is $\gamma = 9.96$ dB, that is a rather large value. If the 17-cell randomizer is used instead of the eight-cell randomizer, leaving unchanged all the other parameters, the value of the power excess becomes smaller, as shown in Figure 12. However, its reduction is not very large: it passes from $\gamma = 9.96$ dB to $\gamma = 6.01$ dB. Indeed, because of the (significantly) larger value of N , the peaks separation is now determined by the value of L resulting in $\Delta = 1$ kHz, that is, quite below the measurement bandwidth.

The problem becomes even more evident if larger values of the bit rate are considered. Table 1 reports the value of γ for increasing values of R_b . We see that a power excess as high as about 12 dB appears for a bit rate of 80 Mbps. Because of the mentioned issues on the simulation complexity, for $R_b = 40$ Mbps and $R_b = 80$ Mbps an observation window $W = 10$ ms has been set, instead of the value $W = 100$ ms used for lower bit rates. The values of γ for the eight-cell randomizer are also reported for the sake of comparison. Actually, the gap between the performance of the two randomizers becomes particularly evident, in absolute terms, for large values of R_b . It is clear that the 17-cell randomizer, though showing a better performance than that of the eight-cell randomizer, is not able to completely remove the problem of high peaks when all-zero OID frames are transmitted at high bit rate. A solution to this problem is proposed next.

4.1 | A method to generate random OID frames

In order to improve the performance of the 17-cell randomizer, reducing the power excess for high values of R_b , we propose to fill the data field of OID frames with the bits generated by another long LFSR.³ The following analysis, in particular, is developed assuming a 32-cell LFSR with primitive polynomial $D^{32} + D^{22} + D^2 + D + 1$. It has period $N = 2^{32} - 1 = 4,294,967,295$ bits. This further random OID generator, which acts only in case of OID frames, should be initialized once per mission (for example with an all-one seed) and then left running.

³This random OID generator has been considered for evaluation at the CCSDS Fall 2019 Meeting in Darmstadt, Germany, on 21–24 October 2019, where an action has been taken to check the agreement of the space agencies in adopting it for future missions.

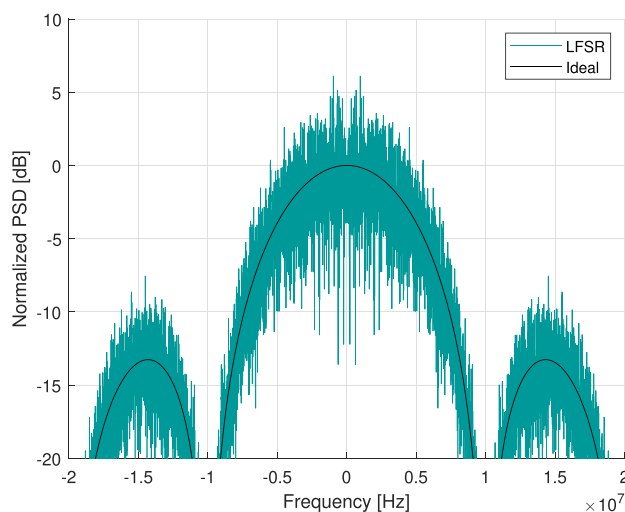


FIGURE 12 Example of power spectrum for a sequence produced by the 17-cell randomizer with $R_b = 10$ Mbps, $L = 10,000$ bits, $B = 4$ kHz, only-idle data (OID) channel access data unit (CADU) with all-zero bits, no attached sync marker (ASM)

TABLE 1 Values of γ for the eight-cell randomizer and the 17-cell randomizer, assuming $L = 10,000$ bits, $B = 4$ kHz, OID CADU with all-zero bits, no ASM and different values of R_b

Bit rate R_b (Mbps)	5	10	20	40	80
Eight-cell randomizer γ (dB)	6.97	9.96	12.96	15.97	18.98
17-cell randomizer γ (dB)	4.66	6.01	6.62	8.69	11.70

Note: $W = 100$ ms for $R_b = 5, 10, 20$ Mbps; $W = 10$ ms for $R_b = 40, 80$ Mbps.

Abbreviations: ASM, attached sync marker; CADU, channel access data unit; OID, only-idle data.

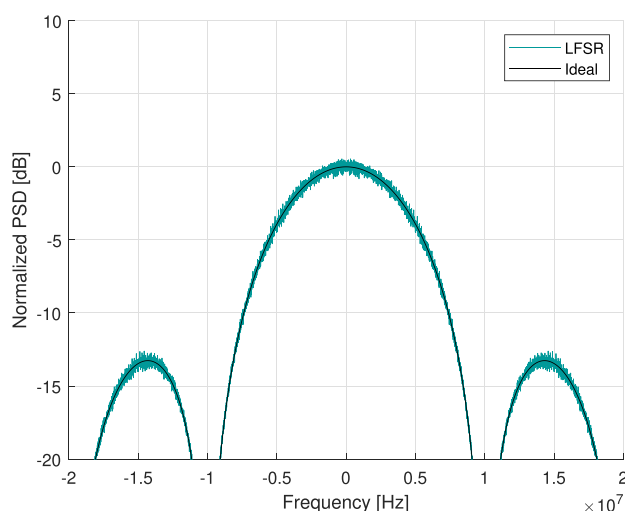


FIGURE 13 Example of power spectrum for a sequence produced by the 17-cell randomizer with $R_b = 10$ Mbps, $L = 10,000$ bits, $B = 4$ kHz, random only-idle data (OID) channel access data unit (CADU), no attached sync marker (ASM)

If the OID frames with all-zero bits are replaced by random OID frames so generated, by using an all-one seed for the random OID generator, the power spectrum in Figure 12 becomes that in Figure 13, where we see that $\gamma = 0.54$ dB, thus quite negligible.

We have verified that using randomly generated bits for OID frames yields benefits also with the eight-cell randomizer, for which the value of γ becomes dramatically smaller as well. Nevertheless, updating the eight-cell randomizer to the new 17-cell randomizer is still advisable, for at least the following two reasons:

- The telemetry TF data field might contain nonrandom segments (this issue will be discussed afterward).
- Legacy compliance is ensured in case nonrandomized all-zero OID frames are still transmitted.

In both these cases, in fact, the 17-cell randomizer is able to limit the power excess, much more than the eight-cell randomizer.

4.2 | Impact of high-order modulations

It must be noted that, besides BPSK, other modulation formats are of interest for space telemetry links. Among them, M -PSK with $M > 2$ and M -APSK, that is, amplitude phase shift keying, according to the constellations and bit mappings described in Consultative Committee for Space Data Systems.¹⁶ Table 2 reports the average and maximum (between brackets) value of γ for some of these modulation schemes over a set of 100 simulations obtained by changing randomly the seed of the random OID generator. Only the 17-cell randomizer is considered. The value of L may be slightly different across modulation formats because we consider sequence lengths that are multiple of the modulation order (e.g., with 64-APSK we have $L = 10,002$ bits). From the table, but also from other results not reported here for saving space, we can conclude that, when random OID frames are transmitted, the 17-cell randomizer is enough to obtain nearly ideal power spectra even when high order modulation formats are considered.

4.3 | Impact of ASM

The presence of the ASM has been neglected in all the above results. In fact, it is qualitatively expected and can be numerically demonstrated that the ASM has a negligible impact in case of long TFs. Such a conclusion, however, might be not so obvious in the case of short frame lengths. For this reason, we report a further set of simulations by assuming $R_b = 10$ Mbps, $B = 4$ kHz, and random OID CADUs, as in Figure 13, but including the ASM and scaling down the value of L from $L = 10,000$ bits to $L = 250$ bits. The obtained values of γ , assuming an all-one seed for the random OID generator, are reported in Table 3. We remind that the total length, L_T , is obtained as $L_T = L + 32$.

From the table, we see that a significant power excess may appear when the frame length L is very short. This is reasonable, because in this case, the ASM, which is a fixed sequence, covers a significant part of the overall sequence with length L_T . On the other hand, the (relatively) high values of γ in Table 3 are also related to the high bit rate. If we assume $L = 250$ bits but $R_b = 1$ Mbps instead of $R_b = 10$ Mbps, maintaining unchanged the other choices, the largest power excess reduces to $\gamma = 1.94$ dB.

TABLE 2 Average and maximum (between brackets) value of γ for high-order modulations, obtained by considering 100 different seeds of the random OID generator

Modulation	4-PSK	8-PSK	16-APSK	32-APSK	64-APSK
γ (dB)	0.52 (0.82)	0.47 (0.79)	0.44 (0.69)	0.44 (0.69)	0.43 (0.80)

Note: The 17-cell randomizer with $L \approx 10,000$ bits, $R_b = 10$ Mbps, $B = 4$ kHz and no ASM is considered.
Abbreviation: OID, only-idle data.

TABLE 3 Values of γ for different frame lengths, including the 32-bit ASM

L (bit)	10,000	1000	500	250
γ (dB)	0.70	1.13	3.24	6.30

Note: Random OID CADU, $R_b = 10$ Mbps, $B = 4$ kHz.

Abbreviations: ASM, attached sync marker; CADU, channel access data unit; OID, only-idle data.

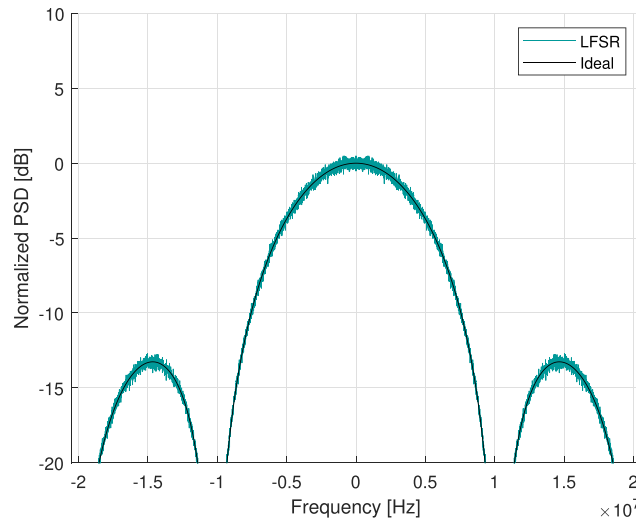


FIGURE 14 Example of power spectrum for a random telemetry (TM) sequence encoded through the low-density parity-check (LDPC) (2048, 1024) code and then randomized through the 17-cell randomizer; $R_b = 10.24$ Mbps, $L = 1024$ bits, $B = 4$ kHz, attached sync marker (ASM) = 32 bits, binary phase shift keying (BPSK) modulation

4.4 | Impact of coding

In the previous sections, we have mainly focused on OID frames. This is because when normal TM data are transmitted they can be usually approximated as random sequences and no significant power excess normally appears. On the other hand, in order to improve reliability, thus reducing the signal-to-noise ratio (SNR) required at the receiver, error correcting codes can be used. Indeed, several options are foreseen by the standards^{5,16,17} including classic codes, like convolutional codes or Reed–Solomon codes, as well as modern codes, like turbo codes or low-density parity-check (LDPC) codes. So, it is interesting to verify that the inclusion of redundancy due to coding does not change the inherent features of the TM information sequences. Actually, in Calzolari et al,¹⁸ we have already proved that, when information sequences are random, turbo-encoded sequences look random as well. In this study, we present a new analysis considering LDPC codes. Figure 14 shows an example of power spectrum for the case of TFs filled with random OID, encoded via an LDPC code with block length $n = 2048$ bits and information length $k = L = 1024$ bits;⁵ the bit rate is $R_b = 10.24$ Mbps, and BPSK modulation is adopted. The ASM is also included. As we see from the figure, the power spectrum is nearly ideal, with a small power excess of $\gamma = 0.65$ dB. We have considered many other operation conditions, basically achieving always the same result: in presence of coding the value of γ obviously changes but remains, in any case, sufficiently small.

4.5 | Almost constant TFs

In this section, we consider TFs filled with nonrandom data that exhibit only small changes for a certain fraction of time. As mentioned in Section 3, some variability is in any case present, because a few bits in the TF header are variable by definition, like frame counters. Consequently, the frame error control field (FECF), optionally applied by means of a cyclic redundancy check (CRC) code at the end of the TF,¹⁵ changes as well. In this case, because all the considered error correcting codes are systematic and the randomizer is restarted at the end of each frame, a quasi-periodicity may appear and this could yield, in principle, a non-negligible power excess. An example is reported in Figure 15, where the frame length and the bit rate are rather large ($L = 10,240$ bits and $R_b = 10.24$ Mbps, respectively). The applied code is again the LDPC (2048, 1024) code. We have verified through simulations that changing few bits in the header of the frame, for example only the frame sequence number, results in a variability of 20 bits or less in the frame, due to the effect of the CRC. However, the impact of the few variable bits is limited, the sequence really looks like quasi-periodic, and a power excess as large as $\gamma = 3.28$ dB may appear.

In this condition, the adoption of the 17-cell randomizer yields significant benefits with respect to the eight-cell randomizer. Figure 16 shows the power spectrum in the same operation conditions of Figure 15 but using the eight-cell randomizer in place of the 17-cell randomizer. As we see, the power excess is now in the order of $\gamma = 9.66$ dB.

It must be noted that transmission of TFs with slowly changing data should only concern low rate channels where, as we have verified, the problem is not relevant. However, our analysis shows that in a hypothetical scenario where almost constant TFs are transmitted at high bit rates, the adoption of a longer randomizer, as the one proposed by NASA, is not enough to solve the power excess problem. A possible solution to

achieve a small power excess in this case consists in changing the rule of restarting the randomizer every CADU. Thus, similarly to what we have proposed for the random OID generator to be used for generating the content of OID frames (described in Section 4.1), the 17-cell randomizer should be initialized once per mission and then left running without restarting. Actually, by applying this strategy, the spectrum in Figure 15 becomes that in Figure 17; here, we have $\gamma = 0.31$ dB, which confirms the effectiveness of such a solution.

Updating of the restarting rule solves the problem of the power excess even in the case of OID frames transmission, thus eliminating the need for the random OID generator. However, while such an approach seems conceptually simple, its practical implementation might be difficult, because of the impact on the synchronization issues. For such reason, the application of this further modification shall be carefully pondered in the future.

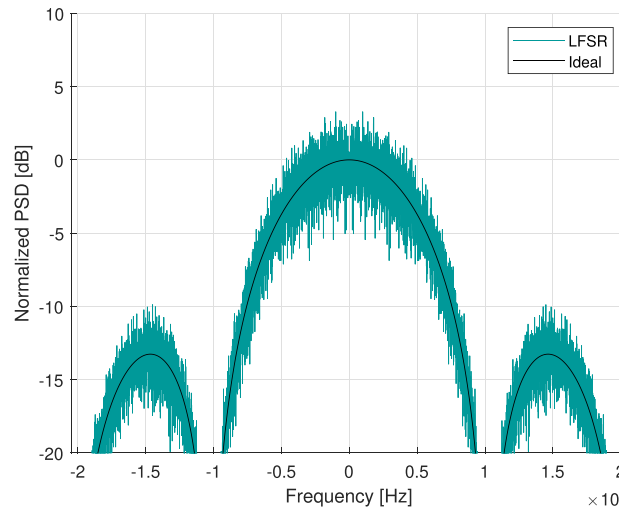


FIGURE 15 Example of power spectrum for a sequence of almost constant transfer frames (TFs) (only the initial 20 bits are variable) encoded through the low-density parity-check (LDPC) (2048, 1024) code and then randomized through the 17-cell randomizer; $R_b = 10.24$ Mbps, $L = 10,240$ bits, $B = 4$ kHz, attached sync marker (ASM) = 32 bits, binary phase shift keying (BPSK) modulation

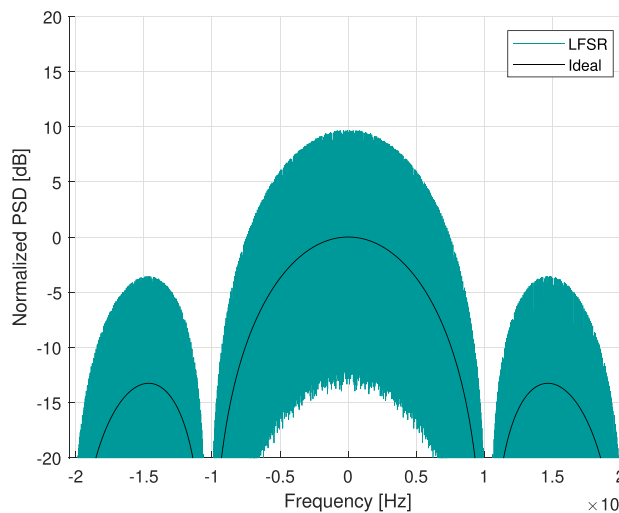


FIGURE 16 Example of power spectrum for a sequence of almost constant transfer frames (TFs) (only the initial 20 bits are variable) encoded through the low-density parity-check (LDPC) (2048, 1024) code and then randomized through the eight-cell randomizer; $R_b = 10.24$ Mbps, $L = 10,240$ bits, $B = 4$ kHz, attached sync marker (ASM) = 32 bits, binary phase shift keying (BPSK) modulation

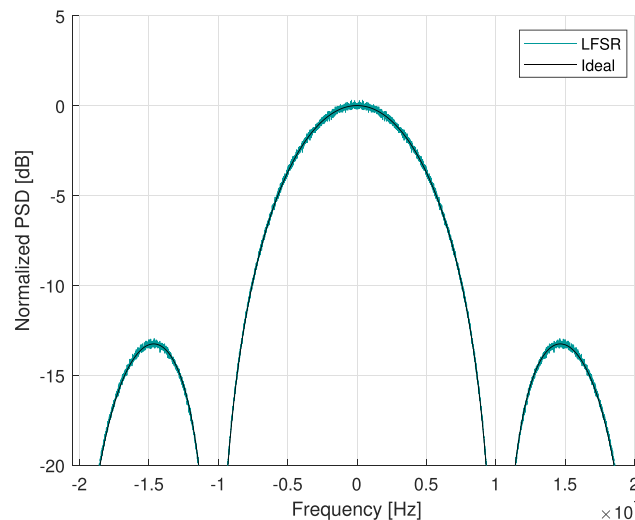


FIGURE 17 Example of power spectrum for a sequence of almost constant transfer frames (TFs) (only the initial 20 bits are variable) encoded through the low-density parity-check (LDPC) (2048, 1024) code and then randomized through the 17-cell randomizer, without reset of the seed; $R_b = 10.24$ Mbps, $L = 10,240$ bits, $B = 4$ kHz, attached sync marker (ASM) = 32 bits, binary phase shift keying (BPSK) modulation

5 | CONCLUSIONS

The main aims of this study have been to quantify the possible violation of ITU PFD limits on the Earth surface due to the transmission of non-random data associated with the CCSDS framing structure and to verify whether a 17-cell randomizer, recently proposed in place of the currently recommended eight-cell randomizer, is able to solve this issue. Not only conventional constant power four-ary and eight-ary modulations but also higher order modulations, up to 64-APSK, have been considered. Our results show that the 17-cell randomizer still has problems with all-zero OID frames, due to the nonideal properties of truncated LFSR sequences.

An effective solution to solve the problem of all-zero OID frames is to fill them with random bits. We have then proposed some simple procedures for the generation of random OID frames by using an asynchronous 32-cell LFSR. We have shown that, if this solution is adopted, both the eight-cell randomizer and the 17-cell randomizer achieve nearly ideal power spectra. Even when such a solution is used, continuing to adopt the 17-cell randomizer may be dictated by the better performance it exhibits in presence of anomalies, like the case of OID frames not properly randomized or almost constant data frames.

We have shown that random OID frames do not exhibit relevant peaks even when high-order modulations, from 4-PSK to 64-APSK, are considered. We have also considered the inclusion of forward error correction coding by assuming LDPC codes. We have verified that, if the bits are random, LDPC encoded frames do not exhibit relevant peaks when the 17-cell randomizer is used. If instead the bits are almost constant, peaks may show up and their amplitude may be significant at high data rates. If almost constant data transmission happens at low data rates, which currently is the most common scenario, this is not an issue; otherwise, the problem is more challenging. A possible solution might be to avoid restarting the randomizer at the beginning of each frame, but this could yield synchronization problems.

In conclusion, our study shows that the use of a 17-cell randomizer and an asynchronous LFSR for filling only-idle frames can provide an effective solution to the spectrum power excess problem, in almost all conditions currently encountered in space telemetry links. Based on the results of this study, CCSDS has started the formal Agency review for incorporating both the asynchronous LFSR and the 17-cell randomizer in the relevant recommended standards.

ACKNOWLEDGMENTS

The authors wish to thank Howard Garon and Victor Sank of NASA/GSFC and Massimo Bertinelli and Andrea Modenini of ESA/ESTEC for fruitful technical discussions on the topic. Open Access Funding provided by Universita Politecnica delle Marche within the CRUI-CARE Agreement. [Correction added on 25 May 2022, after first online publication: CRUI funding statement has been added.]

DATA AVAILABILITY STATEMENT

The data that support the findings of this study are available from the corresponding author upon reasonable request.

ORCID

Roberto Garelo  <https://orcid.org/0000-0003-0292-4648>

REFERENCES

1. Consultative Committee for Space Data Systems (CCSDS). Telemetry summary of concept and rationale, CCSDS 100.0-G-1-S silver book; 1987.
2. International Telecommunication Union (ITU). Radio regulations; 2016.
3. Baldi M, Chiaraluze F, Calzolari GP, Garelo R. Some remarks on the problem of spurious frequencies in high data rate space missions. In: Proceedings 2009 First International Conference on Advances in Satellite and Space Communications (SPACOM). Colmar, France; 2009:107-112.
4. Baldi M, Chiaraluze F, Calzolari GP, Garelo R. Impact of truncation on the statistical properties of LFSR sequences. In: Proceedings International Conference on Signals, Circuits and Systems (SCS 2009); Djerba, Tunisia; 2009:1-6.
5. Consultative Committee for Space Data Systems (CCSDS). TM Synchronization and channel coding 131.0-B-3 blue book; 2017.
6. Alvarez O, Lesthievant G. Pseudo-random codes for high data rate telemetry: analysis and new proposal. In: Consultative Committee for Space Data Systems (CCSDS) RF & Modulation & Channel Coding Working Groups Meeting. Rome, Italy; 2006.
7. European Telecommunications Standards Institute (ETSI). Digital Video Broadcasting (DVB) - Second Generation Framing Structure, Channel Coding and Modulation Systems for Broadcasting, Interactive Services, News Gathering and other Broadband Satellite Applications (DVB-s2), European Standard (Telecommunications series) EN 302 307, V1.2.1; 2009.
8. Baldi M, Chiaraluze F, Boujnah N, Garelo R. On the autocorrelation properties of truncated maximum-length sequences and their effect on the power spectrum. *IEEE Trans Signal Process.* 2010;58(12):6284-6297.
9. Garon H, Sank V. New Longer Randomizer for CCSDS. In: Consultative Committee for Space Data Systems (CCSDS) RF & Modulation & Channel Coding Working Groups Meeting. The Hague, The Netherlands; 2017.
10. Garon H, Sank V. Randomizer for High Data Rates. In: Consultative Committee for Space Data Systems (CCSDS) Coding and Synchronization Working Group Meeting. Gaithersburg, USA; 2018.
11. Garon H, Sank V. Randomizer for High Data Rates. In: Consultative Committee for Space Data Systems (CCSDS) Coding and Synchronization Working Group Meeting. Berlin, Germany; 2018.
12. Abdelaziz M, Fu Z, Anttila L, Wyglinski AM, Valkama M. Digital predistortion for mitigating spurious emissions in spectrally agile radios. *IEEE Commun Mag.* 2016;54(3):60-69.
13. Consultative Committee for Space Data Systems (CCSDS). Radio Frequency and Modulation Systems-Part 1: Earth stations and spacecraft CCSDS 401.0-B-30 blue book; 2020.
14. Consultative Committee for Space Data Systems (CCSDS). Unified space data link protocol CCSDS 732.1-B-1 blue book; 2018.
15. Consultative Committee for Space Data Systems (CCSDS). TM Space data link protocol CCSDS 132.0-B-2 blue book; 2015.
16. Consultative Committee for Space Data Systems (CCSDS). Flexible advanced coding and modulation scheme for high rate telemetry applications CCSDS 131.2-B-1 blue book; 2012.
17. Consultative Committee for Space Data Systems (CCSDS). CCSDS Space link protocols over ETSI DVB-s2 standard CCSDS 131.3-B-1 blue book; 2013.
18. Calzolari GP, Chiaraluze F, Garelo R, Vassallo E. Symbol synchronization properties of CCSDS turbo codes. *Int J Sat Commun.* 2002;20(5):379-390.

AUTHOR BIOGRAPHIES



Massimo Battaglioni (Member, IEEE) was born in Macerata, Italy, in 1991. He received the Laurea degree in electronic engineering, the Laurea Magistrale degree (summa cum laude) in electronic engineering, and the PhD degree in information engineering from Marche Polytechnic University, in 2013, 2015, and 2019, respectively. Since 2019, he has been a Post-Doctoral Researcher with the Department of Information Engineering, Marche Polytechnic University. In 2017, he has been a Visiting Student with the Electrical and Information Technology Department, LTH, Lund University, Sweden. In 2018, he has been a Visiting Student with the Klipsch School of Electrical and Computer Engineering, NMSU, Las Cruces, NM, USA, and with the School of Electrical and Electronic Engineering, University College Dublin, Ireland. His research interests include coding techniques for communications reliability and cryptography, with particular attention to block and convolutional LDPC codes for symmetric and asymmetric channels and their application to cryptography. He also serves as an Editor for IEEE Communications Letters.



Marco Baldi (Senior Member, IEEE) received the Laurea degree (Hons.) in electronics engineering and the PhD degree in electronics, computer, and telecommunications engineering from the Marche Polytechnic University, Ancona, Italy. Since 2019, he has been an Associate Professor with the Department of Information Engineering, Marche Polytechnic University, where he also coordinates the local node of the CINI Cybersecurity National Laboratory and takes part in the Research and Service Center for Privacy and Cybersecurity (CRISPY). He has coauthored more than 150 scientific articles and one book, and he holds four patents. His research interests include coding and cryptography for information security and reliability. He is a member of AEIT, CINI, CNIT, IEEE Communications Society, and IEEE Information Theory Society.

He serves as a Senior Associate Editor for IEEE Communications Letters and an Associate Editor for the EURASIP Journal on Wireless Communications and Networking and the Information Journal (MDPI).



Franco Chiaraluze (Senior Member, IEEE) was born in Ancona, Italy, in 1960. He received the Laurea degree (summa cum laude) in electronic engineering from the University of Ancona, in 1985. Since 1987, he has been with the Department of Electronics and Automatics, University of Ancona. He is currently a Full Professor in telecommunications with the Marche Polytechnic University, Ancona, Italy. He has coauthored more than 300 scientific articles and three books, and he holds three patents. On his research topics, he collaborates with national and international companies. His main research interests include various aspects of communication systems theory and design, with a special emphasis on error correcting codes, cryptography, and physical layer security. He is also a member of the IEICE.



Roberto Garelo obtained a PhD in electronics engineering in 1994 from Politecnico di Torino. Formerly a Professor at the University of Ancona, since 2001, he is an Associate Professor of Communication Engineering at Politecnico di Torino. He visited MIT, ETH, and Cal State LA. His main research topics are channel coding, communication systems, 5G, and space links



Gian Paolo Calzolari received the “Laurea in Ingegneria Elettronica” (Electrical Engineering degree) from the Sapienza University of Rome in 1984. After having worked for the Italian industry (at DATAMAT and ALCATEL-Face Standard Italia), he joined ESA in 1987. At ESOC, he has been involved with definition of requirements, analysis, simulation, system design, and testing of the ESA ground stations equipment on telemetry, telecommand, and channel coding aspects. His work also included advanced studies and international standardisation activities in the field of channel coding, communication protocols, and telemetry/telecommand processing. He is the Area Director for the Space Services (SLS) Area of the Consultative Committee for Space Data Systems (CCSDS) and chairman of the ESA Standardisation Board for Telemetry and Data Handling (STAB). He is also participating in the production of the E-50 series of standards for the European Cooperation for Space Standardisation (ECSS).



Enrico Vassallo (Senior Member, IEEE) was born in Italy in 1959. He received the “Laurea in Ingegneria Elettronica” from Politecnico di Milano, Italy, in 1984. After a short period with the Italian industry, he joined the European Space Agency (ESA) in 1987. Currently, he is the head of ESA frequency management office, in charge of fostering ESA positions at the ITU and CEPT, of the frequency selection, international coordination, and ITU registration of ESA satellites, of obtaining the frequency licenses for ESA stations, and of providing strategic guidance to future ESA projects. His work also includes advanced studies and international standardization activities in the field of radio frequency and modulation and ranging for which he serves as chairman of CCSDS and ECSS. Previously, he worked at ESA as telecommunication engineer for several near earth (Cluster, etc.) and deep space missions (Rosetta, Mars-Express, etc.) and devised the first ESA 35-m antenna station, now part of the three stations ESA deep space network around the world.

How to cite this article: Battaglioni M, Baldi M, Chiaraluce F, Garelo R, Calzolari GP, Vassallo E. Effect of randomizers on the power spectrum excess of space telemetry signals. *Int J Satell Commun Network*. 2022;40(2):67-82. <https://doi.org/10.1002/sat.1416>